Available online at www.sciencedirect.com
ScienceDirect
Journal of Sound and Vibration 300 (2007) 71–87
JOURNAL OF SOUND AND VIBRATION
www.elsevier.com/locate/jsvi

Optimization of multiple edge barriers with genetic algorithms coupled with a Nelder–Mead local search

Marine Baulac*, Jérôme Defrance, Philippe Jean

Centre Scientifique et Technique du Bâtiment, 24 rue Joseph Fourier, 38400 Saint-Martin-d'Hères, France

Received 22 June 2005; received in revised form 17 July 2006; accepted 20 July 2006
Available online 29 September 2006

Abstract

This research work aims at developing a new multi-criteria optimization method dedicated to complex road noise barriers. Numerical simulations of the acoustical propagation have been achieved using MICADO, a 2D boundary element method (BEM) code developed at CSTB. The optimization part is carried out with the help of a Nelder–Mead algorithm (direct local search method) coupled with an evolutionary strategy in order to globalize the approach. A first application of this combination between an outdoor sound propagation numerical code and an optimization algorithm concerns the optimization of noise barrier caps with the following varying parameters: the cap size, its shape and its surface impedance. The cost function to be minimized is defined through a mean value of the insertion loss due to the added crowning compared to the straight, rigid barrier solution of same overall height, averaged on several receiver points within the barrier shadow zone. Final results show a significant improvement of the efficiency of a multiple edge noise barrier by optimizing values of both size and impedance.
© 2006 Elsevier Ltd. All rights reserved.

1. Introduction

More and more noise barriers are built along motorways and railways in order to protect people from transportation noise. Research is constantly evolving in order to improve the performance of such protections taking into account aesthetic and cost points of view. Crownings added at the top of noise barriers have the advantage of improving the barrier performance without increasing its overall height. Many types of complex noise barriers have been proposed within the last decades by manufacturers and acoustics experts. They vary by their shapes or by the materials they are made of. These protections are usually selected according to an empirical approach which consists in imagining a shape and choosing a material and then carrying out tests on a prototype in order to determine the efficiency of the noise abatement device. However, the complexity of the reflection and diffraction phenomena does not make it possible neither to guess in advance which can be the interesting shapes from an acoustical point of view nor where to place the absorbing materials to obtain a maximum efficiency. The 'manual' study of some supposed acoustically interesting cases does not allow a true optimization of an acoustical protection.

*Corresponding author. Tel.: +33 4 76 76 25 35; fax: +33 4 76 44 20 46.
E-mail address: marine.baulac@cstb.fr (M. Baulac).

0022-460X/$ - see front matter © 2006 Elsevier Ltd. All rights reserved.
doi:10.1016/j.jsv.2006.07.030

Here a more systematic analysis is proposed. The purpose of this work is to use an optimization method to directly determine the optimal shapes and impedances and thus to build a noise barrier with a maximum efficiency. The function to be optimized is the average pressure field in a zone to be protected and the optimization variables are the shape and the surface impedance of the acoustical protection. This study is limited to multiple-edge barriers since they are more efficient than classical capped barriers but there are many other possible realistic applications. This paper aims at showing that this kind of optimization allows a noticeable improvement of the performance of the acoustic protection. In the following sections we present the boundary element method for prediction of outdoor sound propagation, optimization algorithms together with the geometrical aspects of this problem. Then results are given and discussed.

2. The boundary element method

The boundary element method relies on the integral equation theory. It has been developed in the 1960s and used extensively to predict sound diffraction by complex impedance discontinuities [1]. Its main advantage is that it allows any kind of shape and impedance condition values on the surfaces to be accounted for in a homogeneous atmosphere.

Two families of boundary element methods can be distinguished: direct and indirect formulations. The direct formulation relies on the use of the Helmholtz integral equation given in Eq. (1) below, where the unknown functions are pressure and velocity. The indirect one is based on an integral formulation assuming that the sound field scattered by a boundary can be represented by a linear combination of a distribution of monopoles (a single-layer potential) and a distribution of dipoles (a double-layer potential).

The numerical code, MICADO, which we propose to use in this work has been developed at the CSTB by Jean [2] and based on the direct integral equation formulation. Here the acoustic pressure $p(M)$ at any point M within Ω should satisfy

$$(\nabla^2 + k^2)p(M) = f(M) \quad \forall M \in \Omega, \tag{1}$$

where $f(M)$ represents the source distribution and k is the wavenumber. As detailed in Fig. 1, a volume D with boundary ξ is included in a domain Ω.

Using the Green's function G and the Sommerfeld condition, the following formula is obtained after mathematical simplifications [1]

$$c(M)p(M) = p_0(M) + \int_{\xi} \left[p(M)\frac{\partial G}{\partial n_S}(S, M) - G(S, M)\frac{\partial p}{\partial n_S}(M) \right] \mathrm{d}S, \ M \in \Omega, \tag{2}$$

where S is a point source at a point $M \in \Omega$, n_s is the normal to the surface σ (notations are detailed in Fig. 1) and c is a coefficient depending on the position of the receiver:

- $c(M) = 1$ for M in the propagation domain Ω except for its boundaries.
- $c(M) = 1/2$ for M on a plane.
- $c(M) = 1-\theta/4\pi$ for an angular point.

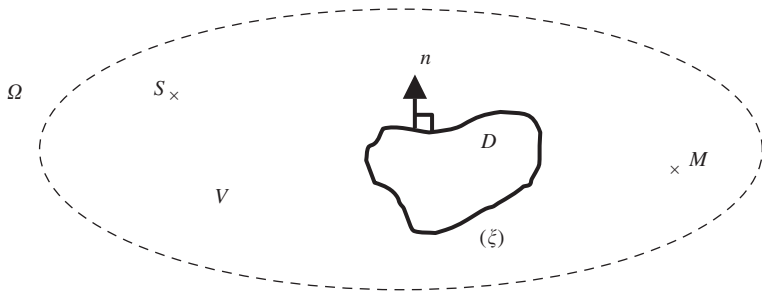

Fig. 1. Notations for the boundary element method.

In MICADO, the BEM is based on a variational approach [2]. The geometry of the problem is 2D: the source is an infinite coherent line source and all the considered configurations remain unchanged and infinite along the direction perpendicular to the vertical section plane (as shown in Fig. 2).

The ground as well as any obstacle surfaces are assumed hard or can be characterized by their own acoustical admittance β, assumed to be locally reactive. The theoretical formalism relies on an integral representation of the pressure field at any point as a function of the pressure on the boundaries, of the admittances as well as of the Green's solution G (elementary solution for a point source M and for a receiver N above an absorbing ground) which can be written as the sum of three different terms [3,4]

$$G(M,N) = -\frac{j}{4}H_0^{(1)}(kr) - \frac{j}{4}H_0^{(1)}(kr') + P_\beta(M,N), \tag{3}$$

where r is the distance between the source and the receiver, r' is the distance between the image-source and the receiver and $H_0^{(1)}$ is the Hankel function of first kind and zero order. The second term in Eq. (3) represents the contribution of the reflection of the cylindrical wave by a perfectly rigid ground and the last term P_β is a corrective factor taking into account the finite ground admittance [3].

BEM calculations have been carried out in this study with a minimum of five elements per segment and per wavelength. This criterion is considered to be high enough for the convergence of calculations with a precision of 0.05 dB in each third octave band.

Although this method can be time consuming, it has proved to be very accurate for computing sound propagation in a homogeneous atmosphere above complex boundaries. This BEM calculation code is used in this project as a black box which is linked to the optimization subroutine discussed in the following section. Simulations of outdoor acoustical propagation are performed on cases with complex noise barriers and optimization algorithms are used to find the best efficiency of such protections.

3. Optimization algorithms

In this section, optimization algorithms used in this study are briefly presented after a short explanation of the choice of those methods.

3.1. The choice of an optimization method

It is necessary to use a direct optimization method since the cost function (defined in Section 4.2) is difficult to differentiate. The Nelder–Mead [5] method (described in next section) has been chosen because of its efficiency in local minimum search. It has been coupled with a stochastic optimization method in order to globalize the optimization. One of the main advantages of this approach is the possibility of optimizing several parameters simultaneously (the dimension of the problem n is the number of parameters to optimize).

The classical method of Nelder–Mead is useful and efficient for unbounded search and local minima investigation. Luersen [6] gives a way to globalize the Nelder–Mead algorithm based on a probabilistic restart procedure that evaluates the probability of having explored a specified region of the domain. Here the globalization is done by several initializations of the Nelder–Mead algorithm in the interval considered. The initializations can be regular, randomized, calculated by a probabilistic restart or induced by a first rough optimization with an evolutionary algorithm [7]. The Nelder–Mead algorithm is applied several times with a different simplex for the beginning in order to explore new regions of the study domain and to find the global minimum of the cost function.

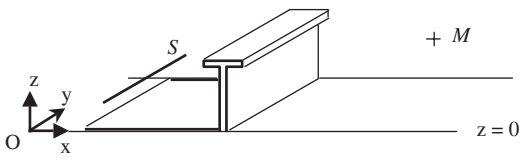

Fig. 2. Geometrical configuration for 2D boundary element method calculations.

3.2. Description of the algorithm of local search: The Nelder–Mead algorithm

The globalization of the Nelder–Mead algorithm is described in Fig. 3.

The Nelder–Mead method attempts to minimize a scalar-valued nonlinear function of n real variables using only function values, without any derivative information (explicit or implicit).

This method has been described for the first time in 1965 [5]. Its starting point is a simplex of dimension $n+1$ where n is the dimension of the problem. A simplex is a Euclidean geometric spatial element having the minimum number of boundary points, such as a line segment in 1D space, a triangle in 2D space, or a tetrahedron in 3D space. The simplex x_i is organized such as: $f(x_1)<f(x_2)<\cdots<f(x_{n+1})$. At each step the worst point of the simplex x_{n+1} is replaced by a new point given by a linear combination between this point itself and the barycentre of the others. The barycenter is the center of gravity or center of mass of the object which means the point representing the mean position of the matter in the object. Main operators are presented in Fig. 4 for a bi-dimensional function. The algorithm stops when the difference between the best point and the worst point of the simplex is smaller than a certain value. Another criterion for the end of the algorithm is the number of function evaluations in order to avoid excessive calculation times.

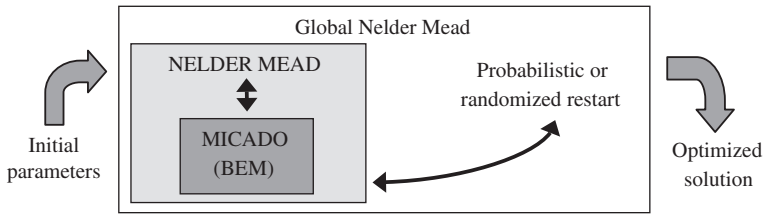

Fig. 3. Principle of the globalization of the optimization.

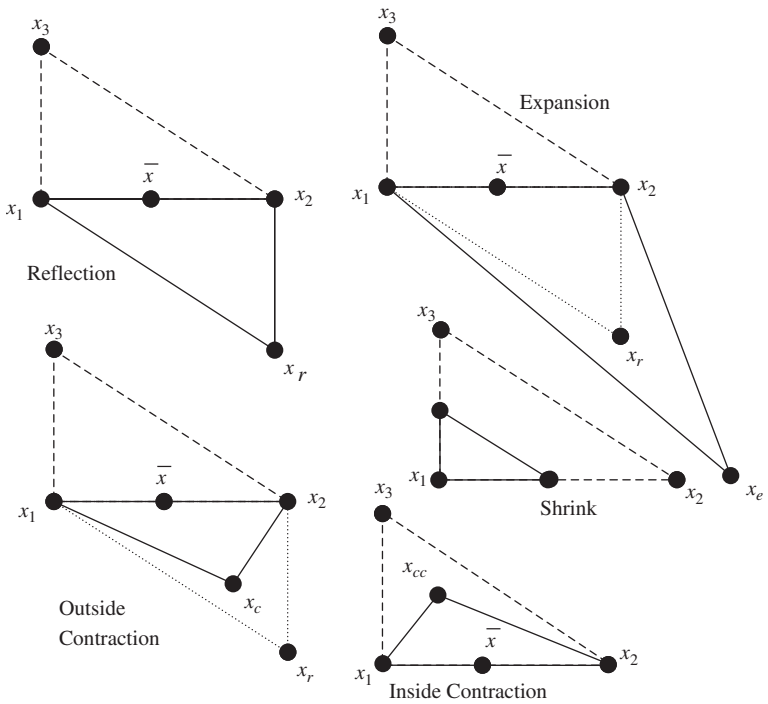

Fig. 4. Main operators of Nelder–Mead algorithm for a bi-dimensional problem.

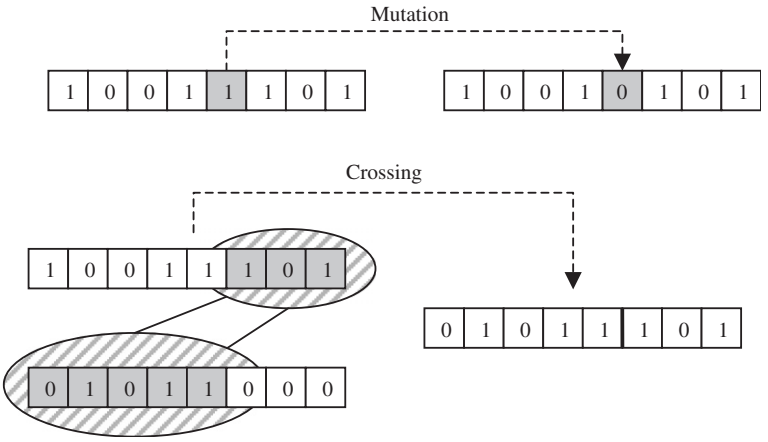

Fig. 5. Principle of mutations (top diagram) and crossings (bottom diagram) with a binary code of variables.

3.3. Modifications of the method

The globalization of the algorithm can be achieved with randomized or probabilistic restarts. When the initializations are randomized, it is a combination of values obtained with the Monte Carlo optimization algorithm [8]. It is not a robust algorithm but it statistically allows exploring the totality of the interval considered. The cost function is evaluated for m points chosen randomly in the interval and the Nelder–Mead algorithm is performed taking the best point as starting point for the simplex. The value of parameter m depends on the number of parameters to optimize. The higher is the number of parameters to optimize, the higher is m in order to increase the probability of exploring the entire studied domain.

Other algorithms used to globalize the optimization are evolutionary algorithms [9]. Here we choose to apply a genetic algorithm or an evolution strategy on a population in order to make a rough optimization; subsequent use of the Nelder–Mead algorithm (taking as starting point the best point found with the evolutionary algorithm) ensures a more precise local search. This coupling between a rough global search and a more precise local search is very efficient for optimizing more than two parameters simultaneously. The basic idea for evolutionary algorithms, such as evolution strategies (ES) [10] and genetic algorithms (GA) [11,12], is to imitate the natural process of biological evolution (Darwinism).

Main characteristics of evolutionary algorithms are:

- a specific representation of candidate solutions of the problem;
- a memorization of results at each stage of the process with the population of elements;
- randomized creation of elements (like mutations defined in Fig. 5, top diagram) which allows the algorithm to explore new region of the study domain;
- a stop criterion for the algorithm (there is no insurance in finding the global minimum);
- operators (like crossings defined in Fig. 5, bottom diagram) for evolution of the population (local search).

One of the simplest and yet powerful evolution strategies is the "one plus one evolution strategy", denoted by (1 + 1)-ES. In this algorithm, both the number of parents and the population size (i.e. number of offspring) are set to one: one parent creates one child. This process can be generalized with the $(\mu + \lambda)$-ES where μ parents create λ children and only the μ best survive. In this work an evolutionary algorithm [13] has been used to do the first rough optimization. Fig. 6 presents the main steps of an evolutionary algorithm.

4. Problem and geometry

This modified algorithm for optimization with the Nelder–Mead method is used to study a quite realistic problem of outdoor sound propagation. The configuration studied is a road represented by one or several

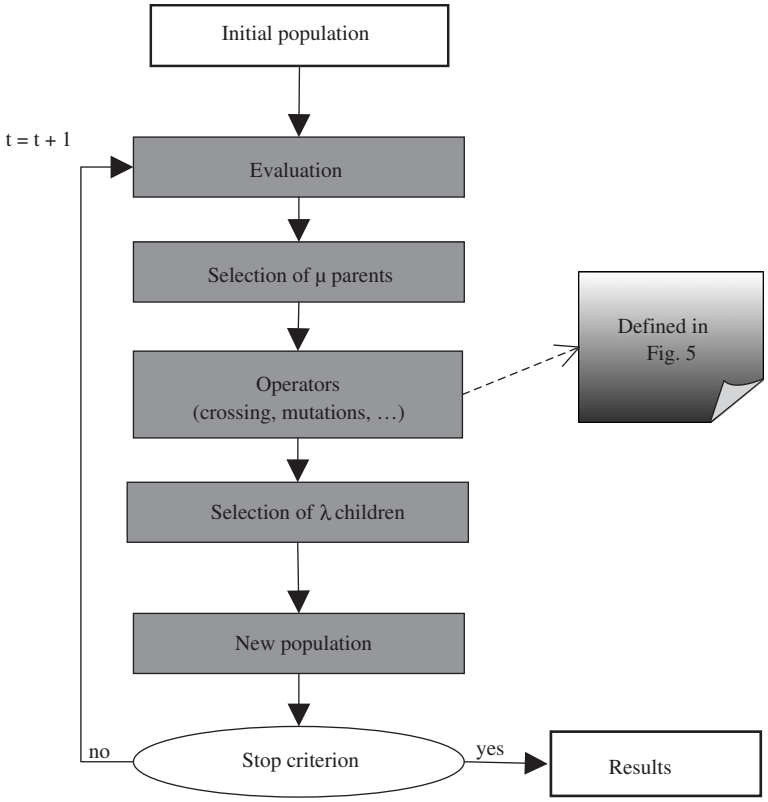

Fig. 6. Principle of an evolutionary algorithm.

infinite line sources, one or several receivers and a complex noise barrier between sources and receivers. The complex noise barriers studied here are rigid straight barriers and multiple edge crowned barriers, all 3-m high. In this section, the geometry of the studied barriers and the source–receiver configurations are first detailed; then the cost function (optimized function) is presented.

4.1. Previous studies

Complex noise barriers have been widely studied; complete reviews and state of the art give an overall view of the topic [14,15]. In order to preserve an aesthetic aspect, diffracting and/or absorbing elements are placed at the top of the acoustic protection. Those crownings improve the performance of the noise barriers without increasing their overall height which often is an important criterion in the acceptance of the protection. In this paper, the studied complex barriers are rigid, straight barriers with lateral edges added; they are called multiple edge barriers (they are described in Fig. 7).

This kind of noise protection device has already been studied, especially by Crombie et al. in 1994 [16] and Watts in 1995 [17–19] but also by other authors like Morgan [20]. It has been shown with numerical simulations that the addition of lateral diffracting edges could increase the efficiency of a rigid straight barrier by up to 5 dB(A) without increasing its height. Scale model measurement have been carried out by Hothersall [21] for railway noise barrier, including some multiple edged barriers. Otherwise, full scale tests [19,22] have been carried out and gave measured efficiencies up to 2.5 dB(A), in a relatively good accordance with theoretical simulations. It is important to note that the performance of such added edges is highly dependent on the source–receiver configuration. Moreover, the importance of source types on efficiencies of caps has been studied at CSTB by Jean et al. [23]; results have shown that the efficiency depends on the choice of source models. There is a number of different shapes of multiple-edge barriers [16]. Here we consider the noise barrier with one lateral edge on each side of the straight barrier, absorbent material only on the two surfaces of the

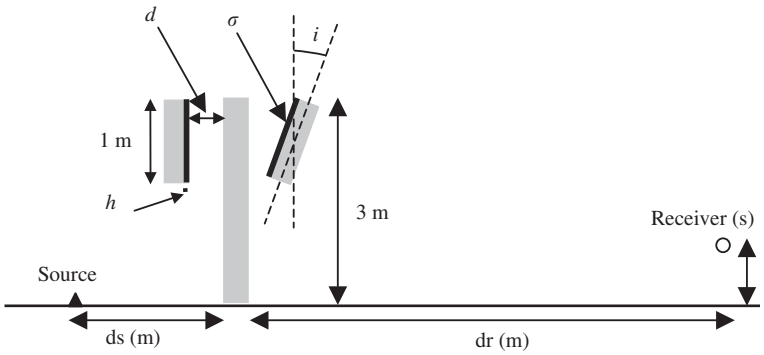

Fig. 7. The four parameters which can be optimized simultaneously: d, σ, h and i.

Table 1
Units and interval of variation for the four parameters

Parameter	Units	Interval	Increment
d	m	[0.2; 3.0]	0.01
σ	kPa s m^{-2}	[1; 20000]	10
h	meters	[0.01; 0.10]	0.01
i	degrees	[−90; 90]	1

lateral edges facing the straight barrier as shown in Fig. 7. Crombie and Watts studied many different shapes of multiple edge profiles but almost always with absorbent surfaces only on the central straight barrier, lateral edges being rigid. Here it is chosen to consider one kind of multiple edge barrier and to try to improve its efficiency by a systematic optimization of some geometrical parameters. Optimization methods have not been widely used to improve the efficiency of road traffic noise protection yet. However in Ref. [24] Thorsson used an optimization method to maximize the efficiency of low height noise barriers with varying surface impedance. He found improvements up to 5 dB(A) but did not consider geometrical parameters in the optimization. Here both shape and surface impedance are optimized.

4.2. Geometry and cost function to optimize

In the present work, the optimization parameters are the shape and the acoustical impedance of the covering material used for the crowning. The impedance is determined by the Delany and Bazley's two parameter semi-empirical model [25]. The two parameters are the flow resistivity σ and the thickness h of the absorbent material. In this work, h is fixed to 0.05 m in most cases while it is specified in the other cases. The ground is chosen perfectly reflective in order to save calculation time; but the method allows to optimize ground impedance characteristics as well.

All capped and straight barriers considered in this paper are 3-m high. The shape parameters are the distance d between the lateral edges and the central rigid straight barrier and the inclination i of those lateral edges. Added panels are 1 m high and 0.1 m thick including absorbing materials; the central straight barrier is also 0.1 m thick. The whole configuration (including added panels) is considered to be infinite and constant in the third direction.

One allows parameters to vary in bounded intervals. The four parameters (defined in Fig. 7) when they are not fixed are optimized inside an interval and with a given increment. The values are recapped in Table 1.

- The distance d between the lateral edges and the central straight barrier can vary from 0.2 to 3.0 m or from 0.2 to 2.0 m according to the studied case. The precision of d is 0.01 m.

Fig. 8. Two configurations: (a) for a positive angle $i>0$; (b) for a negative angle $i<0$.

Table 2
Road traffic noise sound power spectrum: Lw from EN 1793-3:1997

Δf (Hz)	Sound power level of the source: Lw (dB)	Weights from EN 1793-3:1997	$Lw_A(\Delta f)$ (dB(A))
100	110	−20	90
125		−20	90
160		−18	92
200		−16	94
250		−15	95
315		−14	96
400		−13	97
500		−12	98
630		−11	99
800		−9	101
1000		−8	102
1250		−9	101
1600		−10	100
2000		−11	99
2500		−13	97

- The flow resistivity σ is expressed in $1\,\mathrm{kPa\,s\,m^{-2}}$. It can vary from $1\,\mathrm{kPa\,s\,m^{-2}}$ (very absorbent material) to $20{,}000\,\mathrm{kPa\,s\,m^{-2}}$ (rigid material) with a precision of $10\,\mathrm{kPa\,s\,m^{-2}}$. A typical value for mineral wool is $30\,\mathrm{kPa\,s\,m^{-2}}$.
- The thickness h of absorbent materials can vary from 0.01 to 0.1 m and is given with a precision of 0.01 m.
- The inclination i can vary from -90° to $+90^\circ$ (the two configurations for a negative angle or a positive angle are specified in Fig. 8). Angles are given with a precision of 1°.

4.2.1. Sources

Optimizations have been carried out for frequencies spread over a typical road traffic noise frequency range. It has been chosen to carry out the simulations with five frequencies per third octave band since previous calculations have shown that it would be enough for accuracy and convergence of results with a precision of 0.01 dB(A) (it is true for open non-resonant problems only). The global optimization in dB(A) integrates all simulated frequencies from 100 and 2500 Hz third octave bands within the aim of studying realistic cases of transportation noise. Usually in traffic noise studies, calculations are carried out up to 5000 Hz but here preliminary calculations have shown that stopping calculations at 2500 Hz was the best compromise ensuring accurate convergence of results and reasonable calculation time. A typical road traffic noise spectrum given in Table 2 and in Fig. 11 is used for the global calculation of the efficiency. The road traffic noise spectrum used is the A-weighted spectrum calculated with the European standard EN 1793-3:1997 [26]. The influence of the choice of road traffic noise spectrum is shown in Section 5.2.

It is chosen here to consider only one source in all cases of optimization. The source is placed on the ground since the goal in this paper is to demonstrate the feasibility of this coupling optimization method. It is located 8 or 15 m away from the barrier (which are realistic road configurations), according to the studied case, as

shown in Fig. 9. However, several sources could have been considered; in this case, it would have been necessary to sum energetically (incoherent line sources) the contributions of all sources in the calculation of the efficiency.

4.2.2. Receivers

Two kinds of receiver configurations have been chosen as shown in Fig. 9. The first one is with a single receiver located on the ground (in order to eliminate the interference effect between the direct wave and the ground reflection) 32 m after the barrier (top graph (a) in Fig. 9). The second one (bottom graph (b) in Fig. 9) consists of a grid of several receivers located 32 and 100 m away from the barrier at different heights (0, 1, 2, 4, 8, 16 and 32 m above ground). This second configuration allows to consider more realistic transportation noise configurations with receivers at specified altitudes representative of human ears or buildings' floors heights. Here a grid of 14 receivers has been chosen but another receiver configuration could have been selected depending on the area to be protected.

4.2.3. Cost function

The cost function is the name for the function which has to be maximized or minimized in the optimization problem. In our case, the objective is to achieve the maximum efficiency of crowning for a given source–receiver configuration. The cost function is a result of BEM calculations of the efficiency of crowning. It is chosen to do only minimization so the cost function is the global insertion loss $\mathrm{IL}_{\mathrm{global}}$ which is the opposite of the efficiency, and is given by

$$\mathrm{IL}_{\mathrm{global}}(d,\sigma,h,i) = 10\log_{10}\left(\frac{\sum_{\Delta f} 10^{(\mathrm{Lw}_A(\Delta f)+\mathrm{EA}_{\Delta f,\ \mathrm{crowned}}(d,\sigma,h,i))/10}}{\sum_{\Delta f} 10^{(\mathrm{Lw}_A(\Delta f)+\mathrm{EA}_{\Delta f,\ \mathrm{straight}})/10}}\right), \tag{4}$$

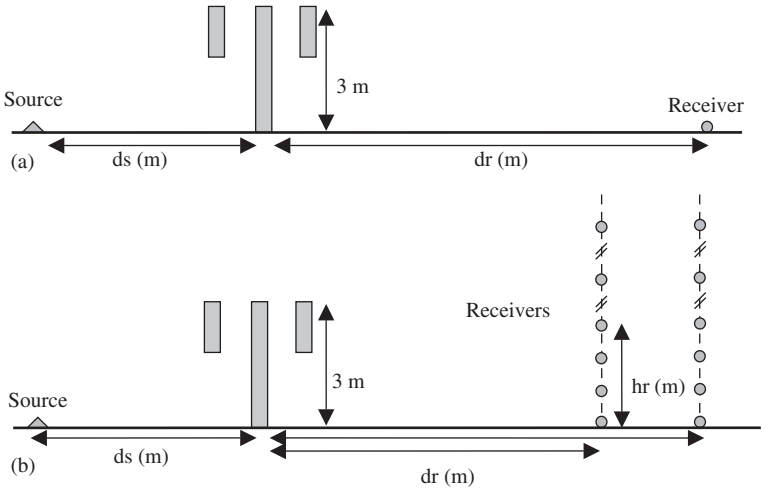

Fig. 9. Two kinds of source and receivers locations. (a): ds = 8 or 15 m; dr = 32 m. (b): ds = 8 m; grid of receivers: dr = 32, 100 m; hr = 0, 1, 2, 4, 8, 16, 32 m.

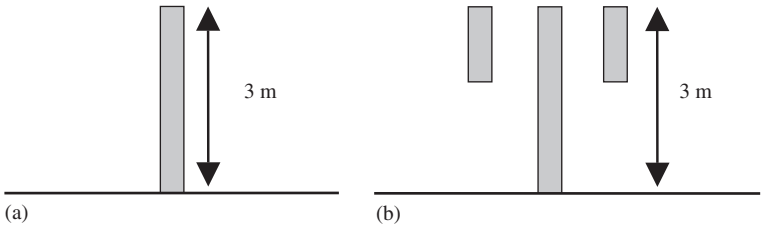

Fig. 10. (a): Straight reference barrier. (b): Multiple-edge crowned barrier.

where $EA_{\Delta f,\ \text{crowned}}$ is the excess attenuation for the capped barrier (referred to free field) and $EA_{\Delta f,\ \text{straight}}$ is the excess attenuation for the 0.1 m thick straight barrier of the same overall height (3 m), as shown in Fig. 10. $Lw_A(\Delta f)$ is the road traffic noise spectrum in third octave bands (Δf) given in Table 2. The lower IL_{global}, the more efficient the noise barrier. Therefore, the aim is to find the minimal IL_{global}.

The cost function does not have an obvious derivative. This is why it has been chosen to use direct optimization methods presented in Section 3. The cost function is also highly dependent on the position and the number of sources and receivers. In configurations where there are several receivers, the cost function calculates the arithmetic average of all the insertion losses calculated for each receiver.

5. Results and discussion

In this section, optimization results of one or more parameter(s) among the four introduced above are presented. Optimizations have been carried out with a criterion for stopping the algorithm when the number of evaluations of the cost function exceeds a certain value.

5.1. Optimization in dB(A) for multiple edge crowning

Table 3 recaps all the results of one- and two-parameter optimization when Table 4 recaps the results of three- and four-parameter simultaneous optimization. Eleven different optimization cases are presented in this section; two others are presented in the next section.

Table 3
Results of different cases of optimization with one or two parameter(s) optimized

Case number	ds	dr	Constrained parameters	Variables	Optimized parameter(s)	Efficiency (dB(A))
Units	m	m	σ in kPa s m^{-2} h in m i in $^\circ$	d in m σ in kPa s m^{-2} h in m i in $^\circ$		
1	8	32	$\sigma = 30$ $h = 0.05$ $i = 0$	$0.2 < d < 3.0$	$d_{\text{opt}} = 0.90$ m	4.5
2	8	32	$\sigma = 100$ $h = 0.05$ $i = 0$	$0.2 < d < 3.0$	$d_{\text{opt}} = 0.94$ m	4.3
3	15	32	$\sigma = 30$ $h = 0.05$ $i = 0$	$0.2 < d < 3.0$	$d_{\text{opt}} = 1.26$ m	4.2
4	8	32 → 100 (grid)	$\sigma = 30$ $h = 0.05$ $i = 0$	$0.2 < d < 3.0$	$d_{\text{opt}} = 2.35$ m	5.0
5	8	32 → 100 (grid)	$\sigma = 30$ $h = 0.05$ $i = 0$	$0.2 < d < 2.0$	$d_{\text{opt}} = 1.89$ m	4.6
6	8	32	$h = 0.05$ $i = 0$	$0.2 < d < 3.0$ $1 < \sigma < 20000$	$d_{\text{opt}} = 0.90$ m $\sigma_{\text{opt}} = 30$ kPa s m^{-2}	4.5
7	8	32	$\sigma = 30$ $h = 0.05$	$0.2 < d < 3.0$ $-90 < i < 90$	$d_{\text{opt}} = 3$ m $i_{\text{opt}} = -31^\circ$	5.3
8	8	32	$\sigma = 30$ $h = 0.05$	$0.2 < d < 2.0$ $-90 < i < 90$	$d_{\text{opt}} = 0.96$ m $i_{\text{opt}} = -23^\circ$	5.2

Table 4
Results of different cases of optimization with three or four parameters optimized

Case number	d*s*	d*r*	Constrained parameters	Variables	Optimized parameter(s)	Efficiency (dB(A))
Units	m	m	σ in kPa s m^{-2} h in m i in $^\circ$	d in m σ in kPa s m^{-2} h in m i in		
9	8	32	$h = 0.05$	$0.2 < d < 2.0$ $1 < \sigma < 20000$ $-90 < i < 90$	$d_{opt} = 0.98$ m $\sigma_{opt} = 30$ kPa s m^{-2} $i_{opt} = -24^\circ$	5.2
10	8	32	$i = 0$	$0.2 < d < 2.0$ $1 < \sigma < 20000$ $0.01 < h < 0.1$	$d_{opt} = 0.90$ m $\sigma_{opt} = 10$ kPa s m^{-2} $h_{opt} = 0.1$ m	5.0
11	8	32		$0.2 < d < 3.0$ $1 < \sigma < 20000$ $0.01 < h < 0.1$ $-90 < i < 90$	$d_{opt} = 1.02$ m $\sigma_{opt} = 10$ kPa s m^{-2} $h_{opt} = 0.1$ m $i_{opt} = -23^\circ$	5.7

5.1.1. One-parameter optimization

The simplest optimization (case 1) is the one-parameter optimization of d, the distance between the lateral edges and the central rigid straight barrier, in the configuration with a single source 8 m away from the barrier and a single receiver located 32 m after the barrier. The other parameters are constrained: $\sigma = 30$ kPa s m^{-2}, h = 0.05 m, $i = 0^\circ$. The algorithm gives the following result: the best efficiency is 4.5 dB(A) and is reached for d equal to 0.90 m.

The second case of optimization is the same as case 1 except the value of constrained flow resistivity which is 100 kPa s m^{-2} instead of 30 kPa s m^{-2}. The optimal efficiency is a bit lower (4.3 dB(A)) and the optimal distance d is nearly the same: 0.94 m instead of 0.90 m.

Case 3 shows the influence of the source location on the optimization results: when the source is located 15 m in front of the barrier instead of 8 m, the maximal efficiency changes from 4.5 to 4.2 dB(A) which corresponds to an optimal distance d of 1.26 m.

Cases 4 and 5 show the influence of considering a grid of receivers instead of a single receiver (details on receivers' locations are given in Fig. 9). Case 4 is a one-parameter optimization of the distance d from 0.2 to 3 m and case 5 is the same but from 0.2 to 2.0 m. The results are an optimal distance d equal to 2.35 m (for an efficiency of 5.0 dB(A)) in the fourth case and an optimal distance d equal to 1.89 m (for an efficiency of 4.6 dB(A)) in the fifth case.

5.1.2. Two-parameter optimization

Cases 6–8 are simultaneous optimizations of two parameters among the four considered in this paper.

Case 6 is the optimization of d and σ simultaneously: the optimal values obtained are a distance d equal to 0.9 m and a flow resistivity σ equal to 30 kPa s m^{-2}; it corresponds to an efficiency of 4.5 dB(A).

Cases 7 and 8 are the optimization of d and i simultaneously.

For case 7, d can vary from 0.2 and 3 m and i from -90 to $+90^\circ$, the optimal values are a distance d equal to 3.0 m (one of the accepted limit) and an inclination i equal to -31° (details about the sign and the inclination are given in Fig. 8), it corresponds to an efficiency of 5.3 dB(A).

For case 8, d can vary from 0.2 to 2 m and i from -90 to $+90^\circ$, the optimal values are a distance d equal to 0.96 m and an inclination i equal to -23°, it corresponds to an efficiency of 5.2 dB(A).

5.1.3. Three-parameter optimization

Cases 9 and 10 are three-parameter optimizations.

Case 9 is the simultaneous optimization of the distance d, the flow resistivity σ and the inclination of lateral edges i. The optimal values are d equal to 0.98 m, σ equal to 30 kPa s m^{-2} and i equal to -24°; it corresponds to an efficiency of 5.2 dB(A).

Case 10 is the simultaneous optimization of the distance d, the flow resistivity σ and the thickness h of absorbent material. The optimal values are d equal to 0.9 m, σ equal to 10 kPa s m^{-2} and h equal to 0.1 m (one of the accepted limit); it corresponds to an efficiency of 5.2 dB(A).

5.1.4. Four-parameter optimization

The last case presented in this section, case 11, is a four-parameter optimization. The optimal values resulting are: a distance d equal to 1.02 m, a flow resistivity σ equal to 10 kPa s m^{-2}, a thickness h of absorbent material equal to 0.1 m (one of the accepted limit) and an inclination i equal to -23°; it corresponds to an efficiency of 5.7 dB(A).

5.2. Influence of the sound power spectrum

It is important to note that the choice of the road traffic noise spectrum has a high influence on the results of the optimization of the parameters. This choice has also an influence on the value of the efficiency of the added edges as it is shown with the comparison of a single parameter optimization with two different spectra. The two road traffic noise spectra used for this comparison are: the one used in previous calculations (calculated with the EN 1793-3:1997 standard and given in Table 2) and another one calculated with the Nord2000 method [27,28] given in Table 5. They are both plotted in Fig. 11.

The results for the single parameter optimization of the distance d between lateral edges and the central rigid straight barrier are given in Table 6. The first line gives the results for the optimization using the road traffic noise spectrum calculated with the EN 1793-3:1997 standard (case 1, presented in previous section). The two following lines (optimization cases 12 and 13) give the results using the Nord2000 road traffic noise spectrum. Case 12 is the optimization of the distance d from 0.2 to 3 m, the optimal value found is equal to 2.35 m, it corresponds to an efficiency of 8.5 dB(A). Case 13 is the optimization of the distance d from 0.2 to 1.5 m, the optimal value found is equal to 0.97 m, it corresponds to an efficiency of 7.5 dB(A). These results show that the choice of the sound power spectrum has an influence on the optimal parameters found and on the best value of the efficiency of the crowning.

Although the resulting efficiency is higher with the second spectrum, the first one had been kept for most of optimization calculations (especially those presented in Section 5.1) because it is calculated with the European standard EN 1793-3:1997.

Table 5
Road traffic noise sound power spectrum: Lw_A from Nord2000 method

Δf (Hz)	Lw (dB) from Nord2000 method	Weights to calculate dB(A)	$Lw_A(\Delta f)$ (dB(A))
100	97.7	−19.1	78.6
125	94.4	−16.1	78.3
160	92.8	−13.4	79.4
200	92.2	−10.9	81.3
250	92.6	−8.6	84.0
315	92.5	−6.6	85.9
400	92.7	−4.8	87.9
500	93.6	−3.3	90.3
630	95.5	−1.9	93.6
800	98.4	−0.8	97.6
1000	101.4	0	101.4
1250	101.7	0.6	102.3
1600	101.3	1	102.3
2000	99.8	1.2	101.0
2500	96.6	1.3	97.9

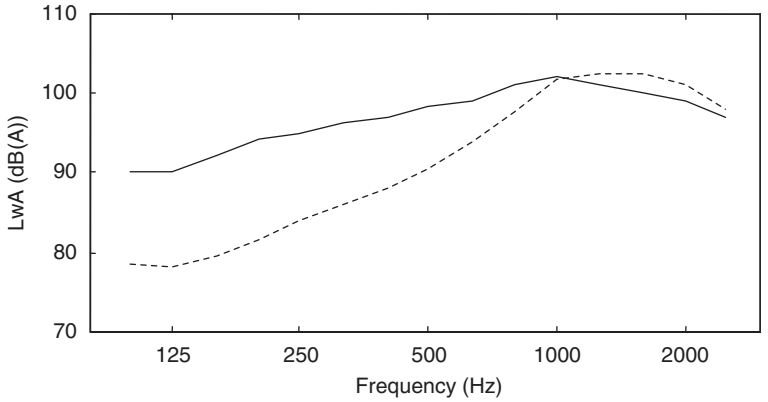

Fig. 11. Comparison of two different road traffic noise spectra. Typical road noise spectrum from European standard EN1793-3:1997 (————) and road noise spectrum of Nord2000 method (- - - - - - -).

Table 6
Results of the influence of the road traffic noise spectrum

Case number	d*s*	d*r*	Constrained parameters	Variables	Optimized parameter(s)	Efficiency (dB(A))
Units	m	m	σ in kPa s m^{-2} h in m i in $^\circ$	d in m σ in kPa s m^{-2} h in m i in $^\circ$		
1	8	32	$\sigma = 30$ $h = 0.05$ $i = 0$ ***EN 1793-3 spectrum***	$0.2 < d < 3.0$	$d_{opt} = 0.90$ m	4.5
12	8	32	$\sigma = 30$ $h = 0.05$ $i = 0$ ***Nord2000 spectrum***	$0.2 < d < 3.0$	$d_{opt} = 2.35$ m	8.5
13	8	32	$\sigma = 30$ $h = 0.05$ $i = 0$ ***Nord2000 spectrum***	$0.2 < d < 1.5$	$d_{opt} = 0.97$ m	7.5

5.3. Global comparison

In this section, vertical noise maps are presented in order to show in a large 2D area the efficiency of multiple-edge noise barriers. The maps comparison allows to show the benefit of the optimization process. Maps have been created taking receivers every 50 cm in both directions x and z (defined in Fig. 2). Previous calculations have shown that it gives accurate maps for those multiple-edge barriers with a precision of 0.05 dB(A). The window considered is 60 m wide (from 10 m before the barrier until 50 m after) and 20 m high (from 0 to 20 m above the ground).

Fig. 12 gives four maps of efficiency resulting of optimization cases 2, 8, 9 and 11 (results and details for each case are given in Tables 3 and 4). It shows the impact of optimizing several parameters simultaneously. Those four maps show that the more parameters are optimized the higher is the final optimal efficiency of the protection.

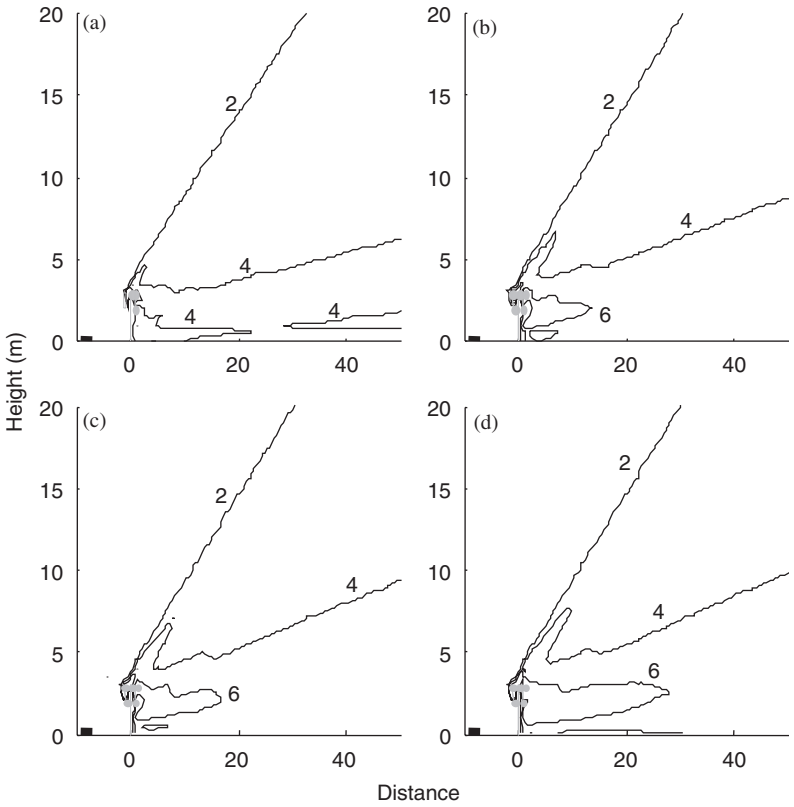

Fig. 12. Influence of the number of optimized parameter. Efficiency of several optimization cases: (a) 1-parameter optimization (case 2); (b) 2-parameters optimization (case 8); (c) 3-parameters optimization (case 9); (d) 4-parameters optimization (case 11).

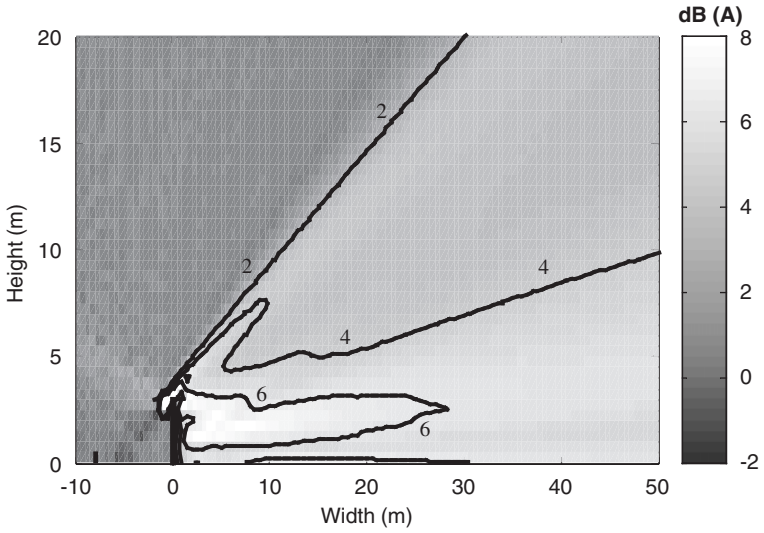

Fig. 13. Map of the efficiency of the multiple-edge crowned barrier with the four optimal parameters. $d = 1.02\,\mathrm{m}$; $\sigma = 10\,\mathrm{kPa\,s\,m^{-2}}$; $h = 0.1\,\mathrm{m}$; $i = -23^{\circ}$.

The noise maps, given in Figs. 13 and 14, represent the efficiency (calculated with Eq. (4)) of two different multiple-edge barriers whose shapes are determined by the four parameters considered in this paper (Fig. 7). Fig. 13 gives the efficiency of the optimal multiple-edge barrier in the following source-receiver configuration:

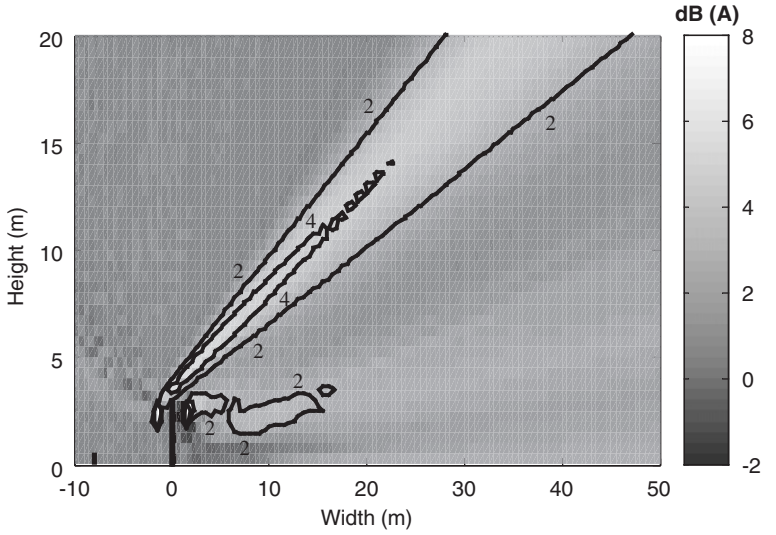

Fig. 14. Map of the efficiency of the multiple-edge crowned barrier with other parameters. $d = 1.5\,\text{m}$; $\sigma = 300\,\text{kPa s m}^{-2}$; $h = 0.05\,\text{m}$; $i = 0^\circ$.

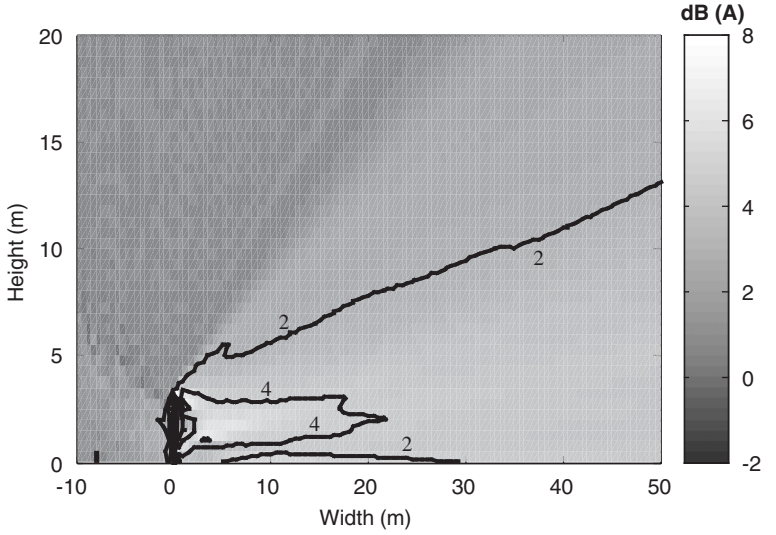

Fig. 15. Map of the efficiency of a multiple-edge crowned barrier previously studied (absorptive materials on the central barrier and rigid lateral edges). $d = 0.5\,\text{m}$; $\sigma = 20\,\text{kPa s m}^{-2}$; $h = 0.1$ m; $i = 0^\circ$.

a single source on the ground, 8 m away from the barrier and a single receiver on the ground and 32 m away behind the barrier. The four optimal values of parameters are those obtained from the four-parameter optimization (case 11 in Table 3) that is to say: $d = 1.02\,\text{m}$; $\sigma = 10\,\text{kPa s m}^{-2}$; $h = 0.1\,\text{m}$; $i = -23^\circ$.

The map in Fig. 13 shows that the optimal multiple edge crowning induces an efficiency up to 6 dB(A) in some parts of the shadow zone and higher than 4 dB(A) in a large area behind the barrier.

Fig. 14 gives the efficiency of another multiple-edge barrier in the source–receiver configuration chosen in order to show the impact of the optimization process. The four parameter values are: $d = 1.5\,\text{m}$; $\sigma = 300\,\text{kPa s m}^{-2}$; $h = 0.05\,\text{m}$; $i = 0^\circ$.

A third global map is given in Fig. 15 for a calculation with parameters chosen in order to fit in with cases of previous studies presented in Ref. [16]. The four-parameter values are: $d = 0.5\,\text{m}$; $\sigma = 20\,\text{kPa s m}^{-2}$; $h = 0.1\,\text{m}$; $i = 0^\circ$. The absorbing materials cover the central straight barrier and lateral edge are rigid.

The comparison between the three maps clearly shows the effect of using optimization algorithm. It is obvious that the optimal multiple edge crowning (Fig. 13) is more efficient than others.

6. Conclusion

An original optimization method coupled with a 2D BEM code has been presented with application to the case of multiple edge barriers. The results show that the lateral edges improve significantly the efficiency of the noise barrier without increasing its height. The improvement reaches more than 6 dB(A) in some parts of the shadow zone. The optimization method chosen has allowed us to optimize several parameters simultaneously and consequently to avoid long and fastidious parametric study of such protections.

Here calculations have been achieved in 2D. It has already been shown [23,29] that in this case tops efficiencies are underestimated in comparison with more realistic 3D simulations: an optimization approach with oblique propagations over the barrier is being developed using a 2D1/2 BEM approach [23,30,31], the main problem still being a high calculation time.

Another important point here is the use of an impedance model [25] which fails at lowest frequencies: some more sophisticated and accurate approaches are being implemented in our optimization code in order to improve the impedance part of it.

Moreover, work is still in progress on other types of complex protections such as random edged barriers and louvred covers, as well as on the introduction in the optimization of other important parameters such as the local aerodynamic conditions above the barrier edge and global meteorological effects. It is also planed to perform scale model measurement in order to validate the results.

Acknowledgement

This work has been carried out within the frame of a Ph.D. thesis supported by a research grant from ANRT and is directed by the Laboratoire de l'Université du Maine (LAUM) and the acoustics and lightening department of Centre Scientifique et Technique du Bâtiment (CSTB).

References

[1] R.D. Ciskowski, C.A. Brebbia, *Boundary Element Methods in Acoustics*, Elsevier Applied Science, London, 1991.
[2] P. Jean, A variational approach for the study of outdoor sound propagation and application to railway noise, *Journal of Sound and Vibration* 212 (2) (1998) 275–294.
[3] S.N. Chandler-Wilde, D.C. Hothersall, Efficient calculation of the green function for acoustic propagation above a homogeneous impedance plane, *Journal of Sound and Vibration* 180 (5) (1995) 705–724.
[4] P. Jean, Y. Gabillet, A boundary element method program to study 2D noise barriers with ground effects, in: Euronoise, Lyon, France, 1995.
[5] J. Nelder, R. Mead, A simplex method for function minimization, *Computer Journal* 7 (4) (1965) 308–313.
[6] M.A. Luersen, R. Le Riche, Globalized Nelder–Mead method for engineering optimization, in: Third International Conference on Engineering Computational Technology, Prague, Czech Republic, 2002.
[7] Z. Michalewicz, *Genetic Algorithms+Data Structures = Evolution Programs*, Springer, Berlin, 1992.
[8] G.S. Fishman, *Monte Carlo: Concepts, Algorithms and Applications*, Springer, Berlin, 1997.
[9] Z. Michalewicz, M. Schoenauer, Evolutionary algorithms for constrained parameter optimization problems, Department of Computer Science, University of North Carolina, Charlotte, USA, 1996.
[10] H.P. Schwefel, *Numerical Optimization of Computer Models*, Wiley, Chichester, UK, 1981.
[11] J.H. Holland, Adaptation in Natural and Artificial Systems, University of Michigan Press, 1975.
[12] D.E. Goldberg, *Genetic Algorithms in Search, Optimization, and Machine Learning*, Addison Wesley, Massachusetts, 1989.
[13] D. Whitley, A genetic algorithm tutorial, Department of Computer Science, Colorado State University, 1993.
[14] I. Ekici, H. Bougdah, A Review of Research on Environmental Noise Barriers, *Building Acoustics* 10 (4) (2003) 289–323.
[15] G.R. Watts, Acoustic performance of traffic noise barriers a state-of-the-art review, in: Eurosymposium on the Mitigation of Traffic Noise in Urban Areas, Nantes, France, 1992.
[16] D.H. Crombie, D.C. Hothersall, S.N. Chandler-Wilde, Multiple-edge noise barriers, *Applied Acoustics* 44 (4) (1995) 353–367.
[17] G.R. Watts, Acoustic performance of a multiple edge noise barrier profile at motorway sites, *Applied Acoustics* 47 (1) (1996) 47–66.
[18] G.R. Watts, Traffic noise barriers, TRL Annual Review, 1995.

[19] G.R. Watts, D.H. Crombie, D.C. Hothersall, Acoustic Performance of New Designs of Traffic Noise Barriers: Full Scale Tests, *Journal of Sound and Vibration* 177 (3) (1994) 289–305.
[20] P.A. Morgan, D.C. Hothersall, S.N. Chandler-Wilde, Influence of shape and absorbing surface—a numerical study of railway noise barriers, *Journal of Sound and Vibration* 217 (3) (1998) 405–417.
[21] D.C. Hothersall, K.V. Horoshenkov, P.A. Morgan, M.J. Swift, Scale modelling of railway noise barriers, *Journal of Sound and Vibration* 234 (2) (2000) 207–223.
[22] G.R. Watts, P.A. Morgan, M. Surgand, Assessment of the diffraction efficiency of novel barrier profiles using an MLS-based approach, *Journal of Sound and Vibration* 274 (3–5) (2004) 669–683.
[23] P. Jean, J. Defrance, Y. Gabillet, The importance of source type on the assessment of noise barriers, *Journal of Sound and Vibration* 226 (2) (1999) 201–216.
[24] P.J. Thorsson, Optimisation of low-height noise barriers using the equivalent sources method, *Acustica—Acta Acustica* 86 (2000) 811–820.
[25] M.E. Delany, E.N. Bazley, Acoustical properties of fibrous absorbent materials, *Applied acoustics* 3 (1970) 105–116.
[26] EN 1793-3. Road traffic noise reducing devices—Test method for determining the acoustic performance—Part 3: Normalized traffic noise spectrum, 1997.
[27] B. Plovsing, J. Kragh, Nord2000. Comprehensive outdoor sound propagation model. Part 1: propagation in an atmosphere without significant refraction. Part 2: propagation in an atmosphere with refraction. DELTA Acoustics & Vibration, Report AV 1849/00 and AV 1851/00, Lyngby, Denmark, 2000.
[28] J. Kragh, B. Plovsing, Nordic environmental noise prediction methods, Nord2000—Summary report. General Nordic Sound Propagation Model and Applications in Source-Related Prediction Methods, DELTA, Acoustic & Vibration, Report AV 1719/01, Lyngby, Denmark, 2001.
[29] J. Defrance, P. Jean, Integration of the efficiency of noise barrier caps in a 3D ray tracing method. Case of a T-shaped diffracting device, *Applied Acoustics* 64 (8) (2003) 765–780.
[30] D. Duhamel, Efficient calculation of the three-dimensional sound pressure field around a noise barrier, *Journal of Sound and Vibration* 197 (5) (1996) 547–571.
[31] D. Duhamel, P. Sergent, Sound propagation over noise barriers with absorbing ground, *Journal of Sound and Vibration* 218 (5) (1998) 799–823.